Available online at www.sciencedirect.com
SCIENCE DIRECT
Journal of Power Sources 153 (2006) 11–17
JOURNAL OF POWER SOURCES
www.elsevier.com/locate/jpowsour

Electrocatalysis of oxygen reduction on carbon supported Ru-based catalysts in a polymer electrolyte fuel cell

R.G. González-Huerta [a], J.A. Chávez-Carvayar [b], O. Solorza-Feria [a,*]

[a] *Depto. Química, Centro de Investigación y de Estudios Avanzados del IPN, A. Postal 14-740, 07360 México D.F., México*
[b] *Instituto de Investigaciones en Materiales, UNAM, México D.F., México*

Received 16 February 2005; accepted 11 March 2005
Available online 3 June 2005

Abstract

Powder of nanosized particles of Ru-based (Ru_x, Ru_xSe_y and $Ru_xFe_ySe_z$) clusters were prepared as catalysts for oxygen reduction in 0.5 M H_2SO_4 and for fuel cells prepared by pyrolysis in organic solvent. These electrocatalysts show a high uniformity of agglomerated nanometric particles. The reaction kinetics were studied using rotating disk electrodes and an enhanced catalytic activity for the powders containing selenium and iron was observed. The Ru-based electrocatalysts were used as the cathode in a single prototype PEM fuel cell, which was prepared by spray deposition of the catalyst on the surface of Nafion® 117 membranes. The electrochemical performance of each single fuel cell was compared to that of a platinum/platinum conventional membrane electrode assembly (MEA), using hydrogen and oxygen feed streams. A maximum power density of 140 mW cm^{-2}, at 80 °C with 460 mA cm^{-2} was obtained for the $Ru_xFe_ySe_z$ catalysts; approximately 55% lower power density than that obtained with platinum.

Keywords: Electrocatalysis; Oxygen reduction; Ru-based cluster catalysts; Cathode; PEMFC

1. Introduction

Fuel cells are becoming a subject of intense applied research. The polymer electrolyte membrane fuel cell (PEMFC) is regarded as a promising high efficiency, low pollution power source for transportation and residential applications [1–6]. A considerable effort has been devoted to the development of fuel cell cathode electrocatalysts to improve their activity and to promote alternatives for reducing the use of noble metal catalysts. Platinum nanoparticles and its alloys are the most common catalysts for polymer electrolyte membrane fuel cells. Electrocatalysis on novel materials for oxygen reduction is an area of interest for electrochemists due to their increasing relevance as cathodic materials in fuel cells, air batteries and industrial electrolytic technology [7–10]. The chemistry of transition metal carbonyl clusters has already been developed in order to prepare highly dispersed molecular compounds, which are supported on different substrates [11], where the reaction of these clusters with elemental chalcogenide generates a variety of polynuclear compounds with coordination center of d-states [12–14]. Oxygen reduction catalysts, which are based on ruthenium molybdenum chalcogenides, were synthesized in xilene [15–17] and dichlorobenzene [18,19] by decacarbonylates of the cluster carbonyls under refluxing conditions for 20 h. Results showed the ability of this type of catalyst to reduce molecular oxygen by a multi-electron charge transfer process ($n = 4e^-$) with water formation. Recently, we have reported the preparation of ruthenium nanoparticles by pyrolysis of dodecarbonyl ruthenium at 220 °C in 1,6-hexanediol under refluxing conditions for 2 h [20]. This synthesized ruthenium catalyst accomplished the direct reduction of molecular oxygen to water in an acid medium, however its catalytic activity is still low compared to that of platinum, the best known electrocatalyst for oxygen reduction.

In this work, the preparation and electrochemical characterization of platinum and ruthenium-based (Ru_x, Ru_xFe_y

* Corresponding author. Tel.: +52 55 5061 3715; fax: +52 55 5747 7113.
E-mail address: osolorza@cinvestav.mx (O. Solorza-Feria).

0378-7753/$ – see front matter © 2005 Elsevier B.V. All rights reserved.
doi:10.1016/j.jpowsour.2005.03.188

and $Ru_xFe_ySe_z$) cluster compounds as cathode electrodes is presented. For electrochemical evaluation, each catalyst was mixed with Nafion® ionomer and Vulcan carbon (VC). The VC and the catalyst were mixed mechanically and impregnated onto an electrode substrate. The oxygen reduction reaction rates were measured using the rotating disk electrode technique. The measured current was corrected for diffusion effects and used to calculate the activity of each catalyst. Electrodes for an MEA were prepared by spraying the catalyst onto the membrane and hot-pressing the gas diffusion electrodes to the polymer membrane. Electrochemical performances involved the study of the temperature effect on the fuel cell.

2. Experimental

2.1. Synthesis of the catalyst

Previous studies in aprotic solvents have reported the synthesis of nanometric particles by descarboxilation of organometallic compounds [20–22]. The nature of the precursor and the solvents in which the chemical reaction is carried out, produce either a high nuclearity carbonyl cluster compound, i.e. $Os_x(CO)_n$ [21], or nanocluster of transition metal chalcogenides, i.e. $W_xRu_ySe_z$ [22]. Nanoparticles of ruthenium were synthesized by reacting 0.135 mM $Ru_3(CO)_{12}$ (Aldrich) in a chemical reactor containing 150 ml of 1,6-hexanediol (bp ≈ 220 °C at 585 mmHg), under refluxing conditions for 2 h. The time was enough to descarboxilate the cluster precursor. Then, the system was cooled down to room temperature and a black powder was precipitated, which was recovered by following a traditional chemical method of separation by adding 50 ml of deionized water to the reactor and 30 ml of ethyl acetate to form two phases which were then separated. The powder was washed with diethyl ether to eliminate the organic reagents and then dried for 20 h at air; afterwards, it was placed in a closed recipient prior to utilization. The same procedure was followed for the preparation of Ru_xSe_y and $Ru_xFe_ySe_z$ nanoparticles where 0.407 mM of elemental Se (Strem) and 0.407 mM $Fe(CO)_5$ (Aldrich) were reacted under refluxing conditions for 2 h.

2.2. Physical characterization

To identify the phases present in the synthesized products, powdered samples were analyzed by XRD technique using a Diffrac Brucker AXS, D8 Advanced Plus Diffractometer. X-ray diffraction patterns were obtained with a step scan of 0.02° 2θ and 9 s per step, between 30° and 90° 2θ, at 35 kV and 30 mA, using Cu Kα radiation, 1.54056 Å. Particle size was determined from transmission electron microscopy (TEM) analyses, with a Jeol JEM 1200 EX microscope, operating at 120 kV and 70 μA. Atomic force microscopy (AFM), using a scanning probe microscope JEOL, JSPM-4210 under normal pressure conditions, in tapping mode, with a resonant frequency in the range 120–190 kHz, and Ultra-Sharp silicon cantilevers NSC 12, was used to study the topography and profiles of the Ru-based samples.

2.3. Electrode preparations and electrochemical set-up

The oxygen reduction reaction (ORR) on the Ru-based cluster electrocatalyst was studied using a rotating disk electrode. Working electrodes were prepared by mixing Vulcan carbon supported catalyst with a Nafion® monomer solution (5 wt%, Dupont). The mixture was sonicated before a small volume (4–8 μl) applied onto the glassy carbon disk with a sectional area of 0.07 cm^2 and then mounted on a concentric Nylamid holder. After drying the ink droplet, at room temperature, a smooth film on the electrode surface was observed. The experimental setup involved a three-electrode arrangement connected to a potentiostat/galvanostat (EG&G model 273A). The reference electrode was Hg/Hg_2SO_4, 0.5 M H_2SO_4 (MSE = 0.67 V/NHE) and the counter-electrode was a platinum mesh. The potentials were referred to NHE. The electrochemical reduction reactions were performed by rotating the catalyst-loaded electrodes at 100–1600 rpm at a scan rate of 5 mV s^{-1} in a 100 ml of 0.5 M H_2SO_4 (pH 0.3) at 25 °C.

Solutions of 0.5 M H_2SO_4 were prepared from double-distilled water and 97.8% H_2SO_4 (Baker analyzed). Prior to electrochemical measurements, the solution was purged with nitrogen for the working electrode activation. During the current–potential measurements, a constant oxygen flux was maintained on the solution surface. The current density was calculated using the geometric surface area of the glassy carbon substrate (0.07 cm^2).

2.4. Preparation of membrane electrode assembly (MEA)

A three layered structure, diffusion, catalyst and monomer layers, was used to prepare the electrodes. Each MEA was prepared by spraying catalyst ink, which contained the cluster catalyst and Nafion® monomer in methanol, on the membrane. 10 wt% Pt/C from E-TEK (Electrochem) was used for the anode catalyst, and synthesized Ru-based catalyst was used for the cathode. The amount of catalyst at the anode was about 0.60 mg cm^{-2} whilst for the cathode was about 0.40 mg cm^{-2}, mixed with 0.6 mg cm^{-2} of carbon powder (Vulcan XC-72, Cabot). After spraying the catalyst onto the membrane, the MEA was heated at 100 °C for 1.5 min. The active area for the anode and cathode was 5 cm^2. The polymer electrolyte membrane was Nafion® 117 (Dupont Fluoro Products), which was treated by consecutive boiling processes for 1 h in 3% H_2O_2, 2 M H_2SO_4 and deionized water, according to the procedure previously described [23]. Before spraying, membranes were dried and flattened.

2.5. Performance evaluation in the PEMFC

The performance of the single cell was evaluated by measuring the *I–E* characteristics of each MEA using an electronic load (Electrochem). The MEA with an active electrode area of 10 cm^2 was coupled with gas-sealing gaskets in a single cell test fixture. H_2 and O_2 (high purity gases) were fed to the single cell under controlled flow rate, humidity, temperature and pressure. Humidification of the reactant gases was carried out by bubbling the gases through water, which was contained in bottles and heated to 5 °C above the temperature of the cell. The fuel cell performance was measured between 40 and 80 °C, at pressures of 30 psi for H_2 and 34 psi for O_2, maintaining a flow rate of 400 $cm^3\,min^{-1}$ in both gases. Measurements were carried out under steady-state conditions.

3. Results and discussion

3.1. Physical characterization

XRD patterns of Ru_x, Ru_xSe_y and $Ru_xFe_ySe_z$ powdered catalysts as-synthesized by pyrolysis of chemical reagents in 1,6-hexanediol are shown in Fig. 1. For all the samples, broad diffraction peaks, which indicate the presence of nanocrystalline powders were observed. Broad humps at the low angle scattering region of XRD patterns suggest that nanosized crystals may be embedded in an amorphous phase product. When only $Ru_3(CO)_{12}$ is pyrolized, the ruthenium powdered catalyst matches well the *JCPDS* standard card 6-663, which corresponds to hexagonal ruthenium [20]. With the addition of Se and $Fe(CO)_5$, additional peaks appear in the XRD patterns maintaining the hexagonal structure of ruthenium as the main structure. No characteristic peaks of Ru, Fe or Se oxides were detected, however these oxides may be present in very small amounts below the detection limit of the equipment or even in an amorphous form. It was observed that the preparation of cluster electrocatalysts by this technique involves complex processes which may led to the formation of low and high-nuclearity cluster compounds.

Fig. 2 shows TEM images of nanosized Ru-based catalysts as-synthesized. These micrographs show a network of spherical and uniformly well-distributed clusters, which are actually composed of agglomerated nanosized particles. On selected areas, the electron diffraction patterns of catalysts show the nanosized particles contain of amorphous and crystalline phases. The TEM image of Ru_x shows particles with a nearly uniform size with an average diameter of about 5 nm. TEM images of Ru_xSe_y and $Ru_xFe_ySe_z$ show that the agglomerated particle size ranges from 50 to 200 nm and consist of fine particles. The electron diffraction patterns of both ruthenium chalcogenide catalysts were composed of concentric rings showing that the diffractions consists of a large number of ultra fine crystalline particles. AFM was used to obtain

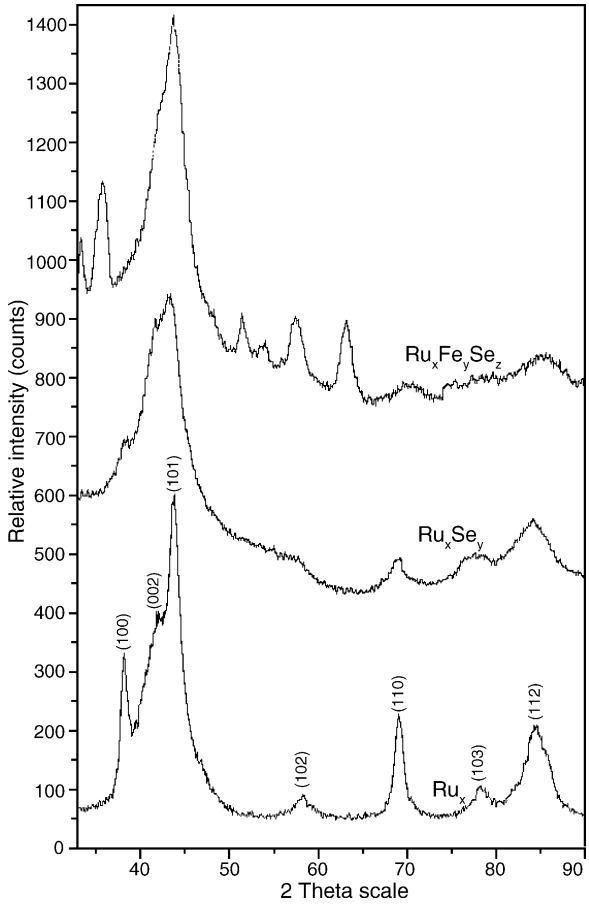

Fig. 1. XRD patterns of Ru_x, Ru_xSe_y and $Ru_xFe_ySe_z$ nanostructured catalysts synthesized by a chemical precipitation reaction in 1,6-hexanediol at 220 °C.

not only the surface morphology of samples but also accurate agglomerate and particle sizes, as shown in Fig. 3. Results showed that agglomerates are in the range 50–250 nm, whilst small particles are ∼1 nm.

3.2. Electrochemical characterization

Polarization curves for oxygen reduction on ruthenium-based carbon supported cluster electrocatalysts were recorded by the linear sweep technique with a sweep rate of 5 $mV\,s^{-1}$ from the potential of 0.85–0.0 V versus NHE, over a range of rotation rates of 100–1600 rpm. The dependence of the reduction reaction as a function of the potential and rotation rate on $Ru_xFe_ySe_z$ cluster catalysts is shown in Fig. 4. Results showed a similar behavior for Ru_x and Ru_xSe_y electrocatalysts, which were reported elsewhere [17,20]. The electrochemical reaction seems to be under kinetic and diffusion control in the range of 0.85–0.40 V. A limiting diffusion current is reached at a higher cathodic potential of 0.40 V/NHE.

Fig. 5 shows typical Tafel plots, which were obtained for the supported Ru-based electrodes in 0.5 M H_2SO_4 solution, under saturated oxygen concentration. Data were corrected

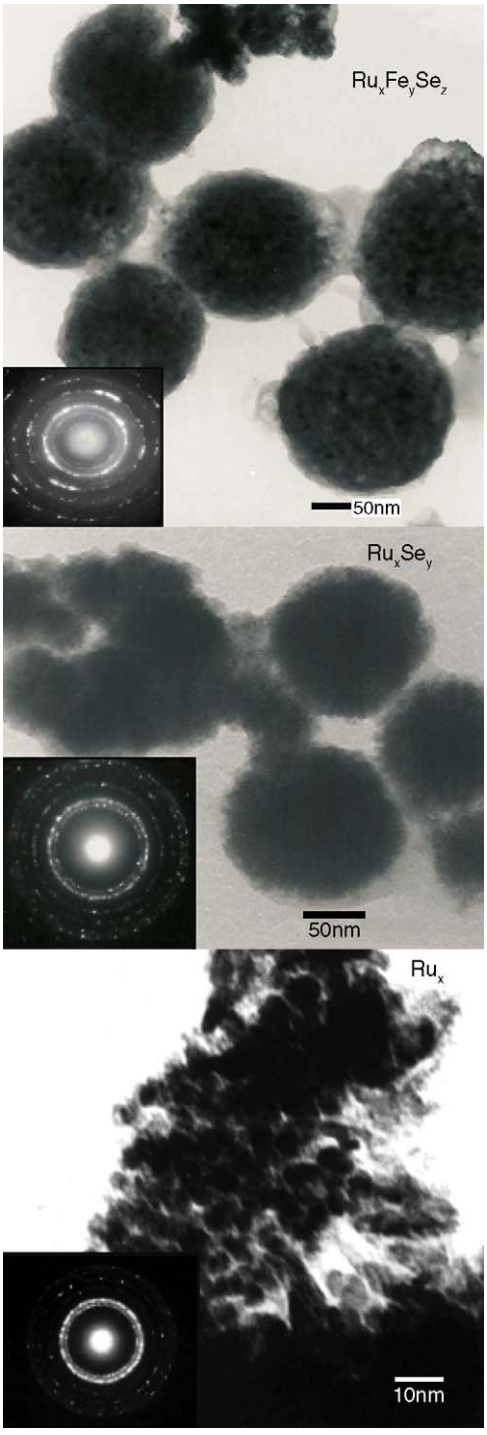

Fig. 2. TEM images and SAD electron diffraction patterns of nanostructured Ru-based catalysts as-synthesized in 1,6-hexanediol at 220 °C.

for diffusion effects using the equation [24]:

$$i_k = \frac{i_L i}{i_L - i}, \quad (1)$$

where i_k, i_L and i are the kinetic, the limiting and the measured currents, respectively. Limiting currents were obtained from a Levich–Koutecky plot, and following a procedure which was

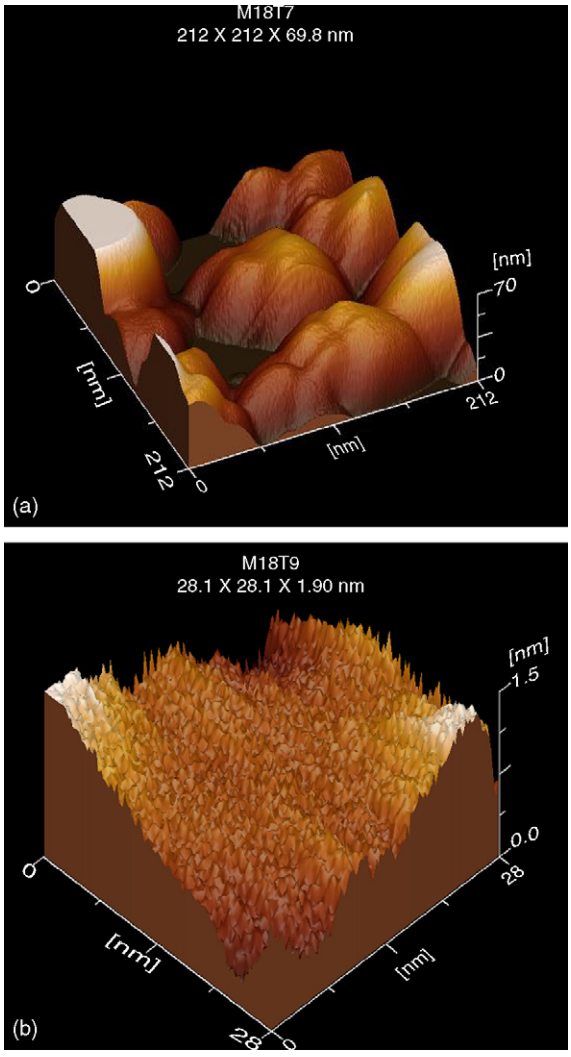

Fig. 3. Surface morphology of $Ru_xFe_ySe_z$ samples obtained by AFM: (a) cluster catalysts and (b) nanometric particles.

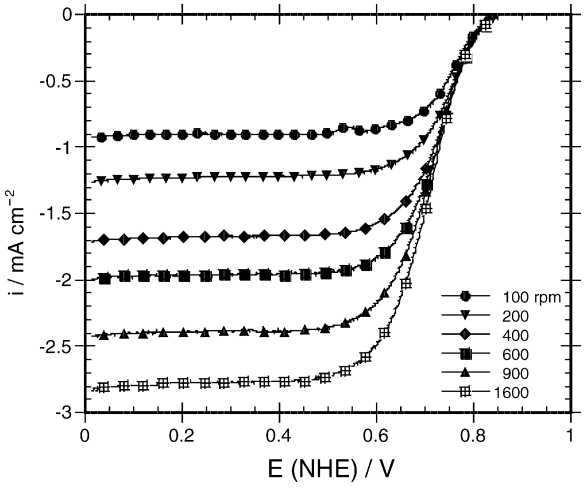

Fig. 4. Oxygen reduction reaction on $Ru_xFe_ySe_z$ electrode at different rotation rates. Oxygen saturated 0.5 M H_2SO_4, sweep rate 5 mV s^{-1}, at 25 °C.

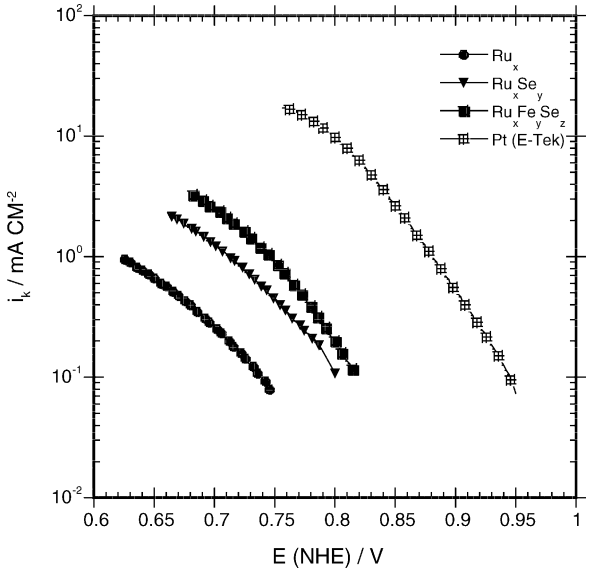

Fig. 5. Mass-transfer corrected Tafel plot for oxygen reduction reaction on Ru-based electrocatalysts in 0.5 M H_2SO_4.

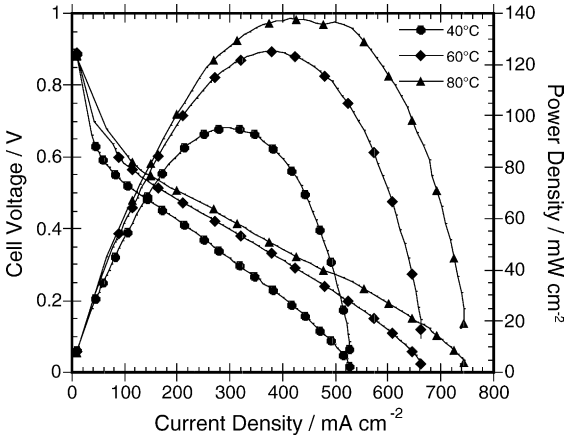

Fig. 6. H_2/O_2 PEMFC polarization curves with as-synthesized $Ru_xFe_ySe_z$ electrocatalyst for oxygen reduction reaction at different temperatures.

described in reference [21]. It may be observed that the presence of selenium and iron strongly enhances the catalytic activities in terms of current densities, compared to those which were obtained with nanometric ruthenium. Tafel slopes were determined in the region where the measured current densities were essentially due to a mixed diffusion-kinetic control for the oxygen reduction reaction. The values of the kinetic parameters, which were determined from data shown in Fig. 5, are summarized in Table 1. The exchange current densities were determined by extrapolation from the linear Tafel region to the reversible potential. A significant improvement in the electrocatalytic behavior in the direction from the nanosized Ru_x to Ru_xSe_y and $Ru_xFe_ySe_z$ cluster compounds was observed. The values of potential, E, which were obtained for $i = 0.1\ A\ cm^{-2}$, are also included in Table 1, where it can be observed that platinum remains as the cathode electrode material with the lowest overvoltage for oxygen reduction. These experimental results are in agreement to the kinetic studies reported on ruthenium-based chalcogenides synthesized in organic solvents for 20 h [17,19].

3.3. Performance testing of membrane electrode assemblies

Since the performance of fuel cells depends on the thickness of the spraying catalyst layer, and to avoid a damage to the membrane, MEAs were prepared by spraying the catalyst directly onto the Nafion® membrane to obtain a layer of an estimated thickness of 20 nm. Then, the catalyzed membrane was sandwiched between two pieces of porous carbon paper electrodes. The MEAs were inserted into the fuel cell for testing processes. To study the temperature effect on the MEA performance, curves of the cell voltage and power density against current density were recorded at 40, 60 and 80 °C with H_2/O_2 under 30/34 psi pressure. Fig. 6 shows the fuel cell performance at different temperatures for the MEA, which was fabricated with a cathode of $Ru_xFe_ySe_z$ cluster catalyst. An improvement of the MEA performance with an increase in the operating temperature was observed. Open circuit voltages, E_{oc}, were around 0.90 V at the operating temperature. Clearly, the measured maximum power density, W_{max}, was 95 mW cm^{-2} at 40 °C, and it increased to 138 mW cm^{-2} at 80 °C, almost 50% higher than the starting current. This fact confirms that the oxygen reduction reaction on $Ru_xFe_ySe_z$ cluster catalyst is activated by temperature, therefore a working temperature higher than 80 °C is needed to enhance the cathodic electrode kinetics and thus the performance of the PEMFC.

When compared with the single PEMFC performance of three cathodes with the same platinum anode catalyst, one may observe the kinetics of the cathode catalyst at the same temperature. Interesting results were obtained when comparing the performance of the $Ru_xFe_ySe_z$ cluster catalyst with those obtained with Ru_x and Ru_xSe_y as cathodes and platinum as the anode in single fuel cells. Fig. 7 and Table 2 show the performances and the parameters determined from

Table 1
Kinetic parameters for ORR in Ru-based cluster catalyst in 0.5 M H_2SO_4

Electrocatalysts	E_{oc} (V/NHE)	$-b$ (V dec^{-1})	α	i_o (mA cm^{-2})	Potential (V) at $i = 0.1$ mA cm^{-2}
Ru_x	0.80	0.110	0.53	4.29×10^{-6}	0.49
Ru_xSe_y	0.87	0.111	0.52	2.22×10^{-5}	0.43
$Ru_xFe_ySe_z$	0.85	0.111	0.51	4.47×10^{-5}	0.41
Pt (10 wt%, E-Tek)	0.96	0.077	0.70	8.47×10^{-5}	0.29

Table 2
Performance of Ru-based cluster cathode catalyst in a PEMFC, at 80 °C, H_2/O_2 under 30/34 psi pressure

Cathodic electrocatalyst	Voltage (V)	W_{max} (mW cm^{-2})	i at W_{max} (mA cm^{-2})	Cell voltage at W_{max} (V)
Ru_x	0.86	70	226	0.31
Ru_xSe_y	0.89	112	329	0.34
$Ru_xFe_ySe_z$	0.88	140	460	0.33
Pt (10 wt%, E-Tek)	0.99	315	656	0.48

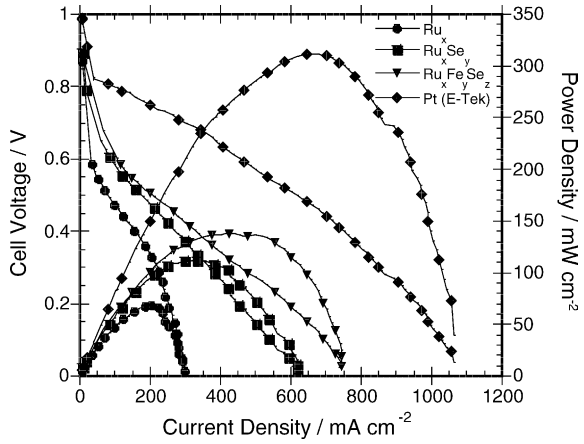

Fig. 7. H_2/O_2 PEMFC performance curves with as-synthesized Ru-based electrocatalysts for oxygen reduction, at 80 °C.

the behavior of the Ru-based cluster catalyst at 80 °C, maintaining the catalyst loading at the anode and cathode as described above. The MEA performance increases as selenium and iron are incorporated into the Ru_x catalyst. In the figure, platinum MEA behavior is depicted. Such a conventional MEA was prepared using the conventional method previously described, with an active area of 5 cm^2 and a catalyst loading of 0.8 mg cm^{-2} (10 wt% Pt/C) on Nafion® 117. The polarization curves of this MEA were measured in the same testing device and tested under the same experimental conditions. It can be observed that the power density obtained with the $Ru_xFe_ySe_z$ cluster catalyst (140 mW cm^{-2} at 460 mA cm^{-2}) is almost 55% lower than that obtained with platinum, under the same experimental conditions. The relatively low output performance observed with the Ru-based chalcogenide catalysts may be attributed basically to the intrinsic properties of the cathodic reaction of the catalysts when they are on polymeric membranes. Additional effort in catalyst preparation and assembly characterizations should be carried out to optimize the cell operation.

4. Conclusions

Ru-based cluster electrocatalysts synthesized by pyrolysis of their carbonyl compounds in aprotic media are suitable materials for the oxygen reduction in acid electrolytes, on cathode electrodes in PEMFCs. The oxygen reduction reaction activity is enhanced in acid media by the incorporation of Fe and Se into the nanometric Ru_x hexagonal phase. In this work, the best performance was obtained with $Ru_xFe_ySe_z$ cluster catalyst with approximately a 55% lower power density than that with platinum.

Acknowledgements

This research project was financially supported by the National Science and Technology Council of Mexico, CONACyT, under Grant No. 41093. The authors wish to acknowledge to Carlos Flores M. for technical assistance. RGGH thanks CONACyT for doctoral fellowship.

References

[1] W. Vielstich, Handbook of Fuel Cells: Fundaments Technology and Applications, vol. 1, John Wiley & Sons, 2003.
[2] M.C. Williams, Fuel Cell Handbook, fifth ed., U.S. Department of Energy, Washington, 2000.
[3] L. Carrette, K.A. Friedrich, U. Stimming, Fuel Cells 1 (2001) 5–39.
[4] J. Larminie, A. Dicks, Fuel Cell System Explained, John Wiley & Sons, 2000.
[5] M.A. Cropper, S. Geiger, D.M. Jollie, J. Power Sources 131 (2004) 57–61.
[6] Q. Li, R. He, J.O. Jensen, N.J. Bjerrum, Chem. Mater. 15 (2003) 4896–4915.
[7] R. Adzik, in: J. Lipkowski, P.N. Ross (Eds.), Electrocatalysis, Wiley/VCH, 1998, pp. 197–244.
[8] A.E. Russell, A. Rose, Chem. Rev. 104 (2004) 4613–4635.
[9] M.L. Perry, T.F. Fuller, J. Electrochem. Soc. 149 (2002) S59–S67.
[10] A.K. Shukla, R.K. Raman, Ann. Rev. Mater. Res. 33 (2003) 155–168.
[11] T.H. Walter, G.R. Frauenhoff, J.R. Shapley, E. Oldfield, Inorg. Chem. 27 (1988) 2561–2563.
[12] A.J. Deening, in: E.W. Abel, F.G.A. Stone, G. Wilkinson (Eds.), Comprehensive Organometallic Chemistry II, vol.7, Pergamon Press, 1995, pp. 683–960 (review 1982–1994).
[13] R.D. Adams, I.T. Horváth, S. Wang, Inorg. Chem. 24 (1985) 1728–1730.
[14] R.D. Adams, Polyhedron 4 (1985) 2003–2025.
[15] O. Solorza-Feria, K. Ellmer, M. Giersig, N. Alonso-Vante, Electrochim. Acta 39 (1994) 1647–1653.
[16] V. Trapp, P. Christensen, A. Hamnett, J. Chem. Soc. Faraday Trans. 92 (1996) 4311–4319.
[17] M. Bron, P. Bogdanoff, S. Fiechter, I. Dorbandt, M. Hilgendorff, H. Schulenburg, H. Tributsch, J. Electroanal. Chem. 500 (2001) 510–517.
[18] O. Solorza-Feria, S. Ramírez-Raya, R. Rivera-Noriega, E. Ordoñez-Regil, S.M. Fernández-Valverde, Thin Solid Films 311 (1997) 164–170.

[19] R. González-Cruz, O. Solorza-Feria, J. Solid State Electrochem. 7 (2003) 289–295.
[20] R.G. González-Huerta, R. González-Cruz, J.A. Chávez-Carvayar, O. Solorza-Feria, J. New Mater. Electrochem. Syst. 8 (2005) 15–23.
[21] O. Solorza-Feria, S. Citalán-Cigarroa, R. Rivera-Noriega, S.M. Fernández-Valverde, Electrochem. Commun. 1 (1999) 585–589.
[22] S.D. Ramírez-Raya, O. Solorza-Feria, E. Ordoñez-Regil, M. Benaissa, S.M. Fernández-Valverde, Nanostruct. Mater. 10 (1998) 1337–1346.
[23] V.A. Paganin, E.A. Ticianelli, E.R. Gonzalez, J. Appl. Electrochem. 26 (1996) 297–304.
[24] A.J. Bard, L. Faulkner, Electrochemical Methods, second ed., Wiley & Sons, 2001.